

Characterization and properties of portland cement composites incorporating zinc-iron oxide nanoparticles

L. MA. FLORES-VELEZ

Laboratorio de Química Ambiental, FCQ-UASLP, 6 Dr. M. Nava, CP78210,
San Luis Potosí/SLP, Mexico
E-mail: florodom@prodigy.net.mx

O. DOMINGUEZ

Departamento de Materiales, IM-UASLP, 550 Sierra Leona CP 78210,
San Luis Potosí/SLP, Mexico

The present work exposes preliminary results concerning ordinary Portland cement (OPC) blended with oxide fumes produced in steel smelting plants and known as electric arc furnace dust (EAFD). After acid treatment of the EAFD, the powder obtained was formed basically of nanometric particles of $ZnFe_2O_4$. The incorporation of EAFD to OPC produced a small retardation of the setting process. Nevertheless, after 7 days the compressive strength of the OPC/EAFD pastes was superior and after 28 days the extent of hydration in OPC and OPC/EAFD pastes was equivalent. The present results indicate that a compressive strength of 72 MPa can be attained after 42 days for OPC doped with 10 wt% of EAFD.

© 2002 Kluwer Academic Publishers

1. Introduction

The densified cement system in which silica fume or microsilica (submicrometer SiO_2 particles) are packed between cement particles, has been widely investigated [1–4]. This material is now commonly referred to as densified with small particles cement. The pozzolanic activity of microsilica is considered to have a significant influence on the microstructure of the system, although particle packing is quite important as well [5]. Microsilica is a by-product of the silicon and ferrosilicon smelting industries. This material in concrete was first tested in Norway in the early 1950s, and intensive research effort near the beginning of 1970s led to the basis of microsilica technology [3].

At present, one of the major waste products of the steelmaking industry is a zinc-iron oxide fume usually known as electric arc furnace dust (EAFD), which is generated in significant volumes and holds the potential for added value if suitable end products could be produced from these powders. Thousands of tons of dust are generated in steel smelting plants each year. Tighter environmental regulations have prompted industry to search new methods of treating waste by-products generated by electric arc furnace during the manufacture of steel. EAFD is considered a hazardous solid waste since it contains small amounts of Pb, Cr and Cd oxides which are evaporated at high temperatures above the steel bath and condensed in the off-gas systems. Because of the extremely fine particles of the powders, one of the possible applications of EAFD could be as reinforcing particles in cement [6].

The present work exposes preliminary results concerning ordinary Portland cement blended with EAFD obtained from steel smelting plants. The study investigate the influence of these nanometric ceramic particles on the hydration reaction as well as the mechanical properties of the blends, exposing a new potential composite material capable of developing high compressive strength.

2. Experimental procedure

Commercial type I ordinary Portland cement (OPC), EAFD from domestic steelmaking industry and distilled water (electrical resistivity 500 Ωm) were used in this study. Before mixing, the EAFD were sieved to remove coarse particles, treated for 24 hours in acid solution (pH 5) and then washed, dried and finally milled for blending. All OPC/EAFD mixes were made using a water/cement ratio of 0.5 and aged at 30°C. The specimens in the same series were tested for compressive strength at the age of 1, 3, 7, 14, 28 and 42 days. The mix proportions of the pastes were made with 2, 5, 8 and 10 wt% of EAFD. In the present work no water-reducing agent or any other chemical compound was added to the OPC/EAFD blends.

Setting time of pastes was determined monitoring the changes in electrical conductivity from samples made of each composition. The cell used to contain the cement paste comprised a cylinder having a diameter of 25 mm and a length of 50 mm. Brass electrodes were attached to the two opposite faces of the cell. The

conductance values were measured using ac voltage 120 Hz and converted to resistivity by the introduction of the cell geometrical constant.

Compressive strengths were measured on samples cast in cylindrical plastic molds having a diameter of 25 and a length of 50 mm. Compressive testing was performed under displacement control using a universal-testing machine with a capacity of 5000 kg. A crosshead speed of $0.76 \text{ mm} \cdot \text{min}^{-1}$ was used. Ten cylinders from each composition were tested for each measurement.

A diffractometer model RIGAKU DMAX with $\text{Cu K}\alpha$ radiation and Ni monochromator was employed at a scanning speed of $0.01^\circ \text{ min}^{-1}$ over the range 2θ from 5 to 90° . Microstructures were examined using a JEOL transmission electron microscopy (TEM) and PHILIPS scanning electron microscopy (SEM) together with an EDAX energy dispersive X-ray spectrometer (EDX). The Fourier transform infrared spectroscopy (FTIR) spectra were recorded using a BRUCKER IFS spectrometer coupled with a photo-acoustic detector MTEC-PHOTOACUSTICS. The FTIR was recorded in the range 6000 to 400 cm^{-1} using 150 scans and obtained at 8 cm^{-1} resolution.

3. Results and discussion

3.1. Starting materials

XRD and EDX were used to determine the oxide and mineralogical compositions of the OPC and EAFD.

Fig. 1 shows that after treatment the EAFD was basically determined as franklinite (ZnFe_2O_4) with smaller amounts of cincite (ZnO) and hematite (Fe_2O_3). EDX analysis carried out on EAFD indicated the presence of small amounts of Pb, Cu, Mn and Cr in the particles. The size, distribution and shape of the EAFD particles were evaluated using SEM and TEM images (Fig. 2). The EAFD was mainly composed of ultra-fine particles presenting spherical shape, generally its size ranging in the nanometric domain. The mean particle size of this fraction of the particles was about 180 nm. Besides, pycnometric measurements carried out on the EAFD indicated a mean apparent density of 4.3 g/cm^3 . XRD patterns were used to obtain approximate estimates of the amounts of unreacted clinker phases and crystallized products. From XRD patterns, the main components of OPC were alite Ca_3SiO_5 (C_3S) and belite Ca_2SiO_4 ($\beta\text{-C}_2\text{S}$) with small amounts of ferrite ($\text{Ca}_2\text{Fe}_x\text{Al}_{2-x}\text{O}_5$) and gypsum ($\text{CaSO}_4 \cdot 2\text{H}_2\text{O}$).

The electrical properties were used as indirect method to monitor the setting of OPC and OPC/EAFD pastes. Fig. 3 shows the electrical resistivity of OPC as a function of time. In this case, the results indicated for the OPC that the setting process started after 4 hours (t_1). Lately, a lack of activity within the paste was observed and the resistivity started to increase once again at 8 hours (t_2), associating this phenomenon to the final setting of the OPC [7].

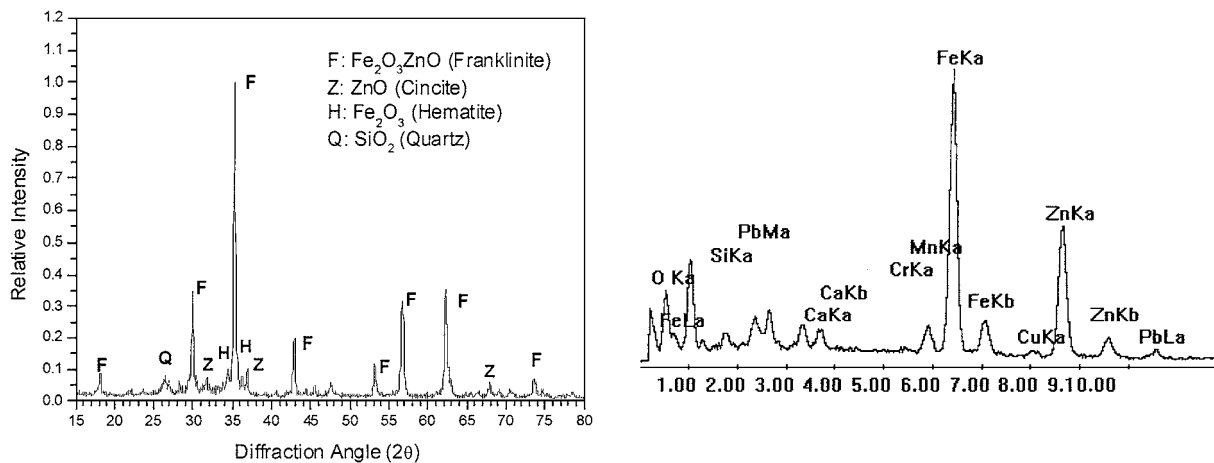


Figure 1 XRD patterns and EDX analysis carried out on the EAFD.

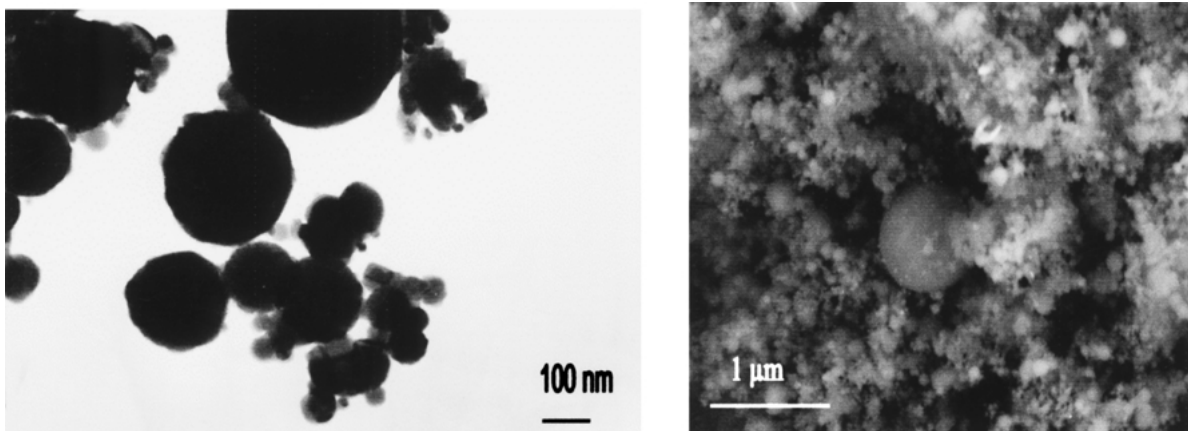


Figure 2 TEM and SEM micrographs obtained from de EAFD showing the presence of spherical nanometric particles.

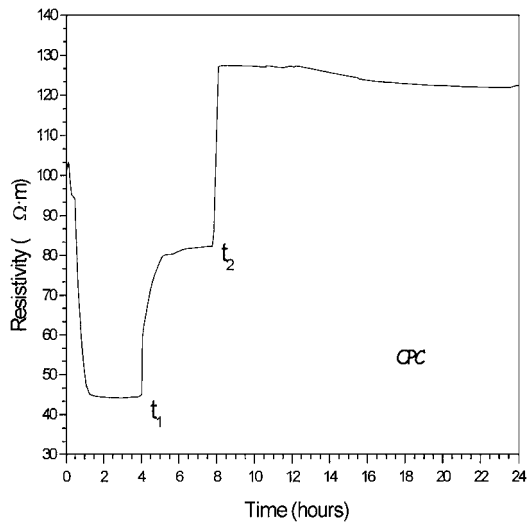
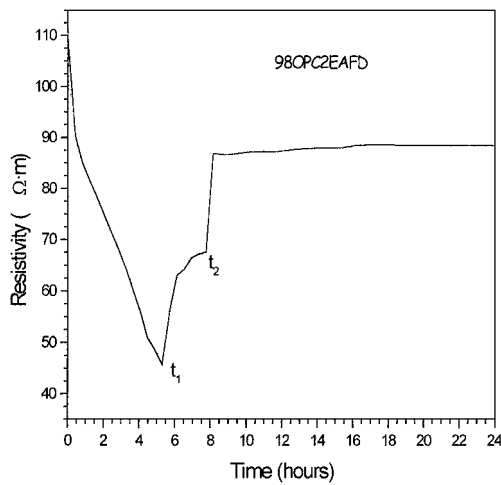


Figure 3 Electrical resistivity as a function of time for OPC paste made with a water/cement ratio of 0.5 and held at 30 C.

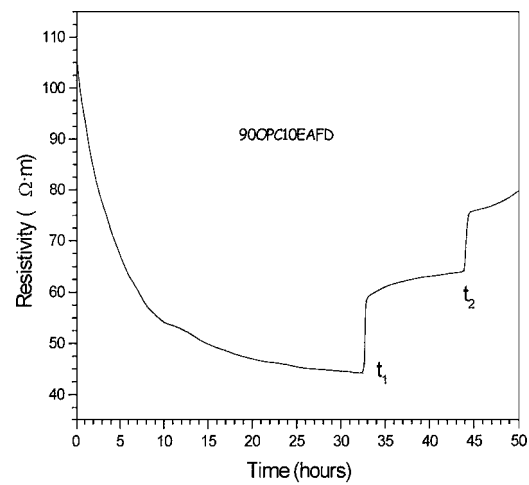
3.2. OPC/EAFD pastes

In order to observe the possible effects of the $ZnFe_2O_4$ compound basically composing the EAFD after chemical treatment, the electrical resistivity of OPC/EAFD blends were used as an indirect method to monitor the

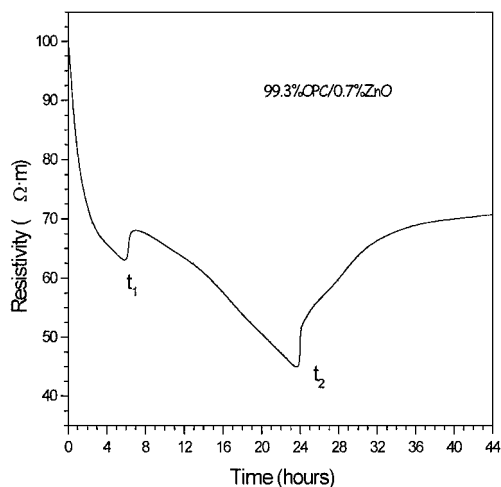
setting reactions. Hydration of Portland cement is a sequence of overlapping chemical reactions and the setting process has been visualized as proceeding through different stages [8]. Information of the degree of hydration has been drawn from monitoring the changes in electrical resistivity of cement pastes [7, 9, 10]. The initial low electrical resistivity immediately after Portland cement is in contact with water has been associated to calcium and hydroxyl ions leached from the clinker, resulting in high ionic concentrations in the bulk aqueous solution [3, 7]. Fig. 4 shows the changes in the electrical resistivity of a OPC paste containing 2 and 10 wt% of EAFD, together with the behavior of OPC/ZnO reference samples. The amount of ZnO in the reference samples was chosen to match the corresponding zinc oxide coming from the $ZnFe_2O_4$ compound incorporated during the addition of the EAFD. The reduction of resistivity of the OPC/EAFD pastes once water was added followed the same trend as the OPC. Nevertheless, there were discernible differences in the setting process, with OPC giving the shortest setting time (Fig. 3), while EAFD doped samples shown different setting times (Fig. 4a and b). It was observed that the setting time of OPC pastes remained almost the same ($t_1 = 5$ hours and $t_2 = 8$ hours) when doped with small amounts of EAFD, indicating that that the addition of



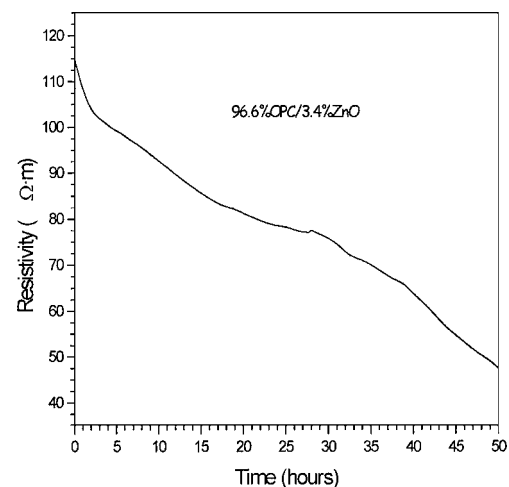
(a)



(b)



(c)



(d)

Figure 4 The electrical resistivity as a function of time obtained from OPC paste containing: (a) 2 and 10 wt% of EAFD; (b) 0.67 and 3.38 wt% ZnO respectively. The w/c ratio in all cases was 0.5 and measurements were carried out at 30°C.

small amounts of EAFD in the OPC pastes did not affect the OPC hydration. On the other hand, once the EAFD content in the OPC paste reaches 10 wt% the setting time attains values of $t_1 = 32$ hours and $t_2 = 44$ hours. Nevertheless, despite the retardation observed, the hydration process takes place contrary to the behavior detected with the OPC/ZnO reference samples, where there is severely failure of the hydration reactions for an equivalent amount of ZnO (Fig. 4c and d).

It is generally accepted that poorly crystalline calcium hydrosilicate phases (CSH) of variable stoichiometries and morphologies together with $\text{Ca}(\text{OH})_2$ are the two most important chemicals formed during the hydration of tricalcium and dicalcium silicates [3, 8]. It is well recognized that some metals in the solid wastes can react with the hydrating cement phases and in some instance cause complete failure of the hydraulic reactions. Much work has already been performed studying the effects of these metals upon OPC hydration, using techniques such as FTIR [11], XRD [12] and SEM [13]. Zinc in different forms (zinc oxide and zinc sulfate) has been understood for many years to delay hydration of cement [14]. Although ZnO severely retards cement hydration during an initial period (Fig. 4c and d), it has also been found to increase the strength at late ages, usually after 28 days [15]. It is believed that during the retardation period a protective cover of an amorphous zinc hydroxide is formed on the grain surfaces. After the retarding effect, high concentrations of Ca^{2+} and OH^- transform zinc hydroxide to crystalline calcium zinc hydroxide $\text{Ca}[\text{Zn}(\text{OH})_3]_2 \cdot 2\text{H}_2\text{O}$ [11].

XRD patterns were used to obtain approximate estimates of the amounts of ZnFe_2O_4 , unreacted C_3S phase and $\text{Ca}(\text{OH})_2$ or $\text{Ca}[\text{Zn}(\text{OH})_3]_2 \cdot 2\text{H}_2\text{O}$ crystallized products. The $\text{Ca}(\text{OH})_2$ production and C_3S consumption can be detected by XRD and have been found to provide a useful means for assessing the extent of hydration [16]. In the present case, there were observable differences in the rate of C_3S consumption as the EAFD content was increased. Nevertheless, it was observed (Fig. 5a) that both OPC and OPC/EAFD samples after 28 days presented equivalent amounts of C_3S and $\text{Ca}(\text{OH})_2$. Since the addition of EAFD did not unduly affect $\text{Ca}(\text{OH})_2$ production in spite of the retardation reactions observed, it is implied that CSH production should be similarly unaffected. On the other hand according to the present knowledge [8, 11], the retardation of the hydration seems to be associated to amorphous zinc hydroxide formed on the grain surfaces together with high concentrations of Ca^{2+} and OH^- leading to crystalline calcium zinc hydroxide $\text{Ca}[\text{Zn}(\text{OH})_3]_2 \cdot 2\text{H}_2\text{O}$. In the present case, XRD patterns obtained after 28 days (Fig. 5b) have only shown the presence of $\text{Ca}(\text{OH})_2$, ZnFe_2O_4 and unreacted C_3S , and the calcium zinc oxide was never detected with the treated EAFD. The lack of peaks associated to the crystallized $\text{Ca}[\text{Zn}(\text{OH})_3]_2 \cdot 2\text{H}_2\text{O}$ could be a consequence of the intrinsic resolution limit of the XRD techniques. In order to surmount this possible effect, FTIR spectroscopy was used to identify the presence of calcium zinc hydroxide. Fig. 6a shows FTIR spectrograms obtained with OPC. Examination of the FTIR

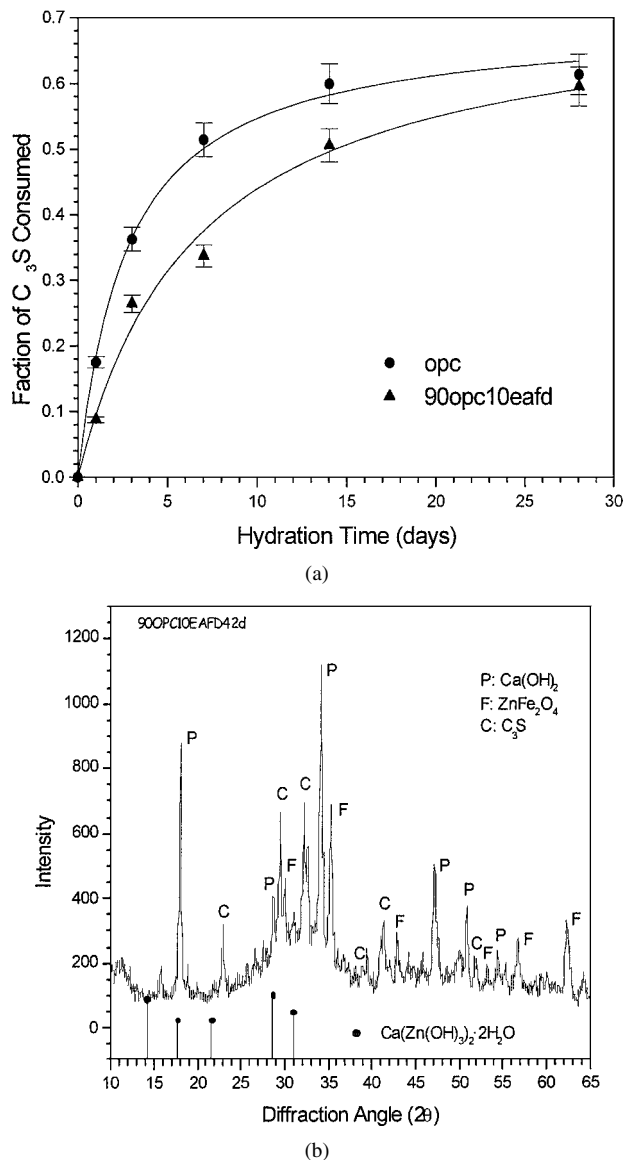
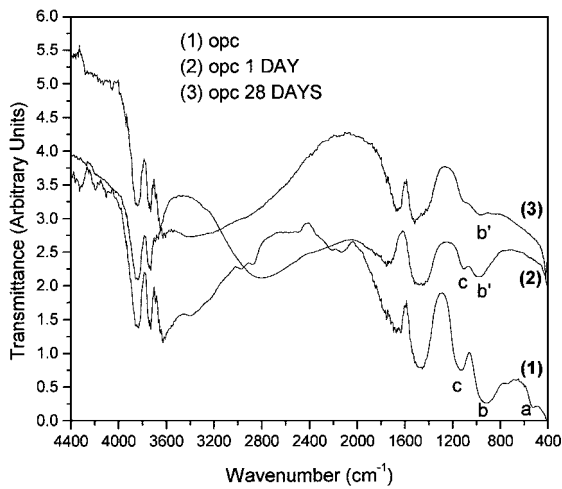
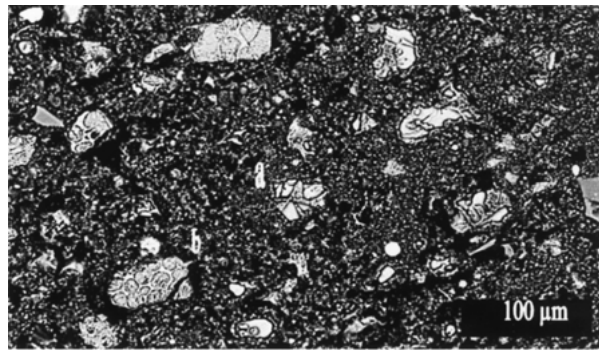


Figure 5 (a) Progress of hydration of tricalcium silicate obtained from OPC and OPC pastes containing 10 wt% of EAFD. (b) XRD pattern obtained after 42 days from an OPC paste containing 10 wt% of EAFD.

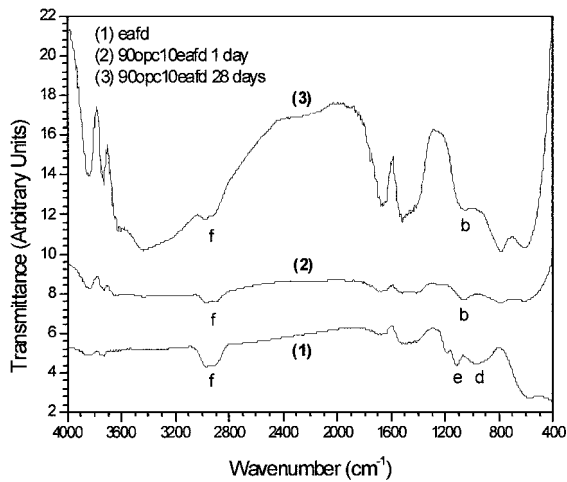
spectra of dry OPC shows the Si—O bending vibrations appearing at 525 cm^{-1} , together with the Si—O asymmetric stretching band due to C_3S and/or $\beta\text{-C}_2\text{S}$ centered at 925 cm^{-1} and the sulfate band (SO_4^{2-}) at 1160 cm^{-1} [11]. Further examination of FTIR spectra of the hydrated OPC shows that the Si—O asymmetric stretching band shifted to higher frequency (960 cm^{-1}) due to the polymerization of the silicates upon setting of the OPC [17]. In contrast, Fig. 6c shows the corresponding FTIR spectrograms obtained with OPC doped with 10 wt% of EAFD after 1 and 28 days. FTIR spectra of hydrated OPC doped with EAFD presents the Si—O asymmetric stretching band shifted to higher frequency (960 cm^{-1}) due to the polymerization of the silicates together with a strong absorption band observed for EAFD at 2900 cm^{-1} . It has been reported in the literature [11] a strong absorption band in the 3650 cm^{-1} zone for the $\text{Ca}[\text{Zn}(\text{OH})_3]_2 \cdot 2\text{H}_2\text{O}$ compound. In this case, there was no evidence of the strong absorption band at 3650 cm^{-1} associated to the calcium zinc hydroxide. Besides, the absorption band at



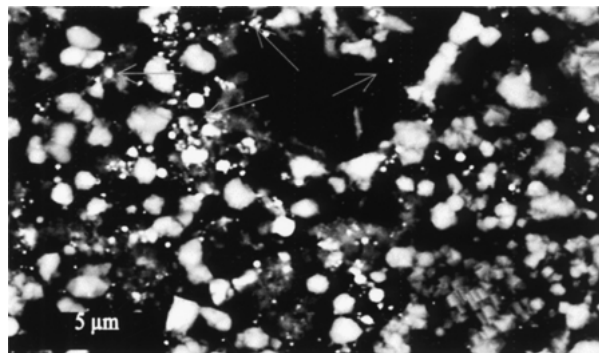
(a)



(b)



(c)



(d)

Figure 6 FTIR spectra obtained with (a) opc at different hydration times and (c) 90opc10eafd pastes at different hydration times. Photograph (b) concerns the microstructure observed with sample 90opc10eafd after 42 days where letters a and b represents unreacted grains of alite and belite. Photograph (d) is an enlargement obtained from the same sample where the arrows point to ZnFe_2O_4 particles.

2875 cm^{-1} corresponding to ZnFe_2O_4 was observed even after 28 days. The present results suggest that no discernable reaction takes place between OPC and the ZnFe_2O_4 and if occasionally weak bands were observed between 3600 and 3800 cm^{-1} , they should be associated to $\text{Ca}[\text{Zn}(\text{OH})_3]_2 \cdot 2\text{H}_2\text{O}$ coming from the reaction between Ca^{2+} and the small amount of ZnO still present in the EAFD. On the other hand, SEM images (Fig. 6b and c) obtained from 90OPC10EAFD sample after 42 days indicates the presence of the nanometric particles of the EAFD immersed in the CSH matrix even at this stage of hydration, suggesting that probably there is no reaction between the Zn^{2+} forming the ZnFe_2O_4 and the Ca^{2+} and OH^- ions, or it should occur at a lower rate on the surface of the particles. Nevertheless, further studies have to be carried out to properly know the chemical processes involved in these composite pastes, specially the leaching rate of Zn^{2+} from the ZnFe_2O_4 crystal lattice.

Just as in other structural material, the mechanical properties play a relevant role and the achievement of higher strength has been one of the final goals in cement based materials. Concerning cement pastes and concrete, physicochemical and mechanical properties

like durability, wear resistance, strength, permeability to water and gases, ionic diffusion, cracking, etc. are all important to fully characterize the final material. Nevertheless, compressive strength is probably the most important parameter used to describe the potential improvement made in the material. Traditional hardened cement pastes are porous and complex solids where the microstructural nature of Portland cement-based products gives rise to time-dependent mechanical properties [3, 8]. Concerning the effect of the ZnFe_2O_4 nanometric particles on the mechanical properties of cement, the strength of the hardened cement-doped pastes was determined. Fig. 7 shows the curves of compressive strength versus hydration time obtained from OPC and OPC/EAFD pastes. It was observed that cement doped with 2 and 5 wt% had since the beginning of the hydration process greater strength than the control cement. On the other hand, the addition of more than 5 wt% of EAFD to cement depress the strengths before day 3, but increases it drastically after 7 days. This behavior is a consequence of the delay in the hydration process observed when OPC is doped with EAFD (Fig. 4). Despite the retardation of strength, cement doped with EAFD presents

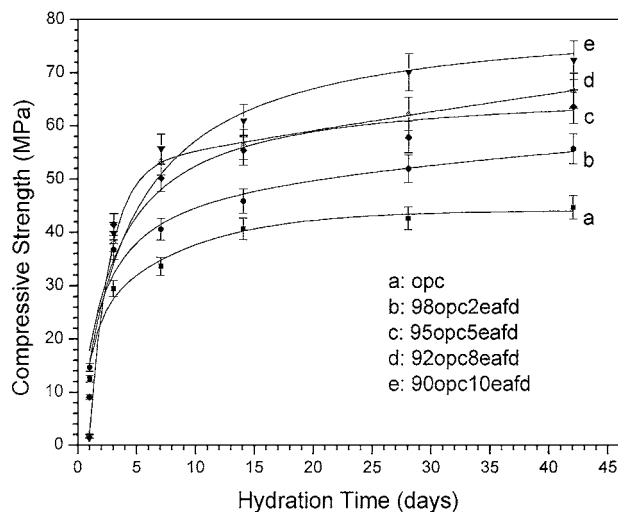


Figure 7 Compressive strength results for different mixtures of cement and EAFD.

an interesting time-dependent mechanical behavior. It has been established that ZnO severely retards cement hydration during an initial period, but it has been found by other studies to increase the strength at late ages (28 days and more) [3, 8, 15]. After retardation, here again the strength follows acceleration and finally achieves higher compressive strength than OPC pastes. Fig. 7 indicates that the EAFD can improve the compressive strength from 40 MPa for ordinary Portland cement to 72 MPa for the OPC paste doped with 10 wt% of EAFD. Considering that concrete containing 5 to 15% silica fume attain high compressive strength, up to 100 MPa [1–4], the present results suggest the potential capability of the OPC/EAFD pastes to become a new cement particle composite formulation.

4. Conclusions

A relevant aspect of the electric arc furnace dust (EAFD) concerns the particle size of this powder, usually formed by particles in the nanometric domain. X-ray diffraction confirms that after acid treatment, the amount of zinc in the oxide form (ZnO) is reduced while zinc-iron oxide ($ZnFe_2O_4$) is the predominant compound forming EAFD. It was observed certain delay in the setting process of cement as the EAFD content was increase, nevertheless the hydration reactions seem to take place as in OPC after 3 days. A compressive strength of 72 MPa was attained after 42 days for OPC doped with 10 wt% EAFD. This value is quite similar to the limit strength usually reported for equivalent OPC pastes doped with silica fume. Fur-

ther research has to be undertaken to fully characterize the OPC/EAFD composites, specially those concerning physicochemical properties and durability. From the environmental point of view, the leaching of heavy metals from the composites will have to be quantified in order to defined the proper chemical processing of the EAFD and the final composition of the composites. At present there is not enough information to estimate the cost and handling problems associated with this new component, nevertheless, the present preliminary results suggest that OPC/EAFD pastes could have the potential to become a new cement particle composite formulation.

Acknowledgment

Authors grateful acknowledge CONACyT for the financial support granted to this project.

References

1. H. ASGEIRSSON and G. GUDMUNDSSON, *Cem. Concr. Res.* **9** (1979) 249.
2. D. M. ROY, *Science* **235** (1987) 651.
3. P. C. HEWLETT, "LEA's Chemistry of Cement and Concrete," 4th ed. (Arnold, London, 1998) p. 675.
4. V. M. MALHOTRA (ed.), "Fly Ash, Silica Fume, Slag and Natural Pozzolans in Concrete," Proceedings Fifth International Conference, Milwaukee Wisconsin, USA (1995).
5. D. M. ROY, Z. E. NAKAGAWA, B. E. SCHEETZ and E. L. WHITE, *Mater. Res. Soc. Symp. Proc.* **42** (1985) 245.
6. O. DOMINGUEZ, Mexican Patent, pending.
7. W. J. MC CARTER and A. B. AFSHAR, *Cem. Concr. Aggregates* **7**(2) (1985) 57.
8. H. F. W. TAYLOR, "Cement Chemistry," 2nd edition (Thomas Telford Publishing, 1997).
9. M. A. TAYLOR and K. ARULANANDAN, *Cem. Concr. Res.* **4** (1974) 881.
10. E. KARMAZSIN and M. MURAT, *ibid.* **8** (1978) 553.
11. M. Y. A. MOLLAH, T. R. HESS, Y. TSAI and D. L. COCKE, *ibid.* **23** (1993) 773.
12. H. F. W. TAYLOR, K. MOHAN and G. K. MOIR, *J. Amer. Ceram. Soc.* **68**(12) (1985) 680.
13. S. A. RODGER and G. W. GROVES, *ibid.* **72**(6) (1989) 1037.
14. G. D. FOWLER, S. ASAVAPISIT, C. R. CHESSMAN and R. PERRY, in Actes du Congrès International Sur Les Procédés de Solidification et de Stabilisation de Déchets, Nancy-France, 28 Nov.–1 Dec., 1995, edited by J. M. Cases and F. Thomas (Société Alpine de Publications, Grenoble, France) p. 40.
15. I. W. HAMILTON and N. M. SAMMES, *Cem. Concr. Res.* **29** (1999) 55.
16. H. F. W. TAYLOR, K. MOHAN and G. K. MOIR, *J. Amer. Ceram. Soc.* **68**(12) (1985) 685.
17. J. BENSTED and S. P. VARMA, *Cem. Technology.*, September/November (1974) 440.

Received 27 December 2000

and accepted 22 October 2001